Nonresonant Optical Activity of Isolated Organic Molecules

Shaun M. Wilson,[†] Kenneth B. Wiberg,[†] James R. Cheeseman,[‡] Michael J. Frisch,[‡] and Patrick H. Vaccaro*,[†]

Department of Chemistry, Yale University, P.O. Box 208107, New Haven, Connecticut 06520-8107, and Gaussian, Inc., 340 Quinnipiac Street, Building 40, Wallingford, Connecticut 06492

Received: August 2, 2005; In Final Form: October 12, 2005

Cavity ring-down polarimetry (CRDP) has been exploited to interrogate the nonresonant optical activity (or circular birefringence) of prototypical organic compounds in the vapor phase, thereby revealing the *intrinsic* chiro-optical response evoked from *isolated* (solvent-free) molecules. Specific polarization rotation parameters have been measured at two distinct excitation wavelengths (355 nm and 633 nm) for a variety of gas-phase species drawn from the terpene, epoxide, and alkane/alkene families, with complementary solution-phase polarimetric studies serving to highlight the pronounced influence of solute−solvent interactions. Time-dependent linear response calculations performed at high levels of density functional theory have been enlisted to unravel the structural and electronic origins for observed behavior. Aside from elucidating the complex solvation processes that mediate chiro-optical phenomena taking place in condensed media, this study affords a critical assessment for emerging ab initio predictions of nonresonant optical activity and for their promising ability to assist in the determination of absolute molecular stereochemistry.

I. Introduction

The chiral nature of molecules and the stereospecificity of molecular interactions play pivotal roles in diverse fields of physical, chemical, and biological importance,[1,2] ranging from fundamental investigations of parity nonconservation[3] and asymmetric catalysis[4] to the interminable quest for the origins of life.[5] A key issue for all of these endeavors is determination of the absolute configuration for a targeted species, as defined most commonly by elaborating the three-dimensional arrangement of substituents about each stereogenic center. Two venerable methods have emerged for accomplishing this crucial task *directly*, X-ray diffraction analyses[6] (which demand high-quality crystalline samples as well as additional phase information deduced from anomalous dispersion effects) and rational total syntheses[2] (which can be time-consuming, labor intensive, and costly). *Indirect* strategies, including those based on X-ray characterization of diastereomeric crystals[2] or clever magnetic resonance[7] and mass spectrometric[8] procedures, have been shown to be of considerable utility; however, their fruitful application requires the controlled action of supplementary (chiral) complexation agents that must bind selectively to the molecule of interest. The inherent difficulties and limitations of these schemes have motivated substantial efforts to identify alternative means for discriminating chiral structure, particularly in systems where pronounced conformational flexibility or unusual bonding motifs preclude the use of established techniques. Recent years have witnessed the rapid development of chiro-optical spectroscopy[9−11] for the in situ assignment of absolute molecular configuration, with the complementary vibrationally mediated probes of Raman optical activity[12] (ROA) and vibrational circular dichroism[13] (VCD) found to be especially promising. The concerted experimental and theoretical work reported in this paper focuses on the related phenomenon of nonresonant optical activity,[9,11,14] ultimately striving to transform such facile polarimetric measurements into versatile tools for the extraction of (absolute) stereochemical information.

Electromagnetic radiation propagating through a chiral medium experiences a complex index of refraction ($\eta = n + i\kappa$) that differs in both real ($\Delta n = n_L - n_R$) and imaginary ($\Delta\kappa = \kappa_L - \kappa_R$) parts for the two polarization states comprising the helicity (or circular) basis.[9,11] The resulting phenomena of circular birefringence (CB for $\Delta n \neq 0$) and circular dichroism (CD for $\Delta\kappa \neq 0$) lead to observable effects in the form of nonresonant (linear) polarization rotation and resonant (circular) differential absorption, respectively, which are connected formally through extension of the canonical Kramers−Kronig relationships.[11] The molecules (of opposite handedness) that comprise an enantiomeric pair long have been known to display wavelength-resolved optical activities (CB and CD) of equal magnitude but inverse sign, thereby affording a facile means for their relative discrimination.[10] Unfortunately, the a priori correlation of a specific chiro-optical response (sign as well as magnitude) with an individual enantiomer still presents formidable challenges, usually requiring supplemental chemical results and/or semiempirical models to reach a definitive assignment. While the basic theoretical framework governing chiral matter-field interactions was established at the dawn of quantum mechanics,[15,16] reliable computational methods for predicting molecular optical activity are just beginning to emerge.[14,17−37] Such ab initio calculations are crucial for the extraction of stereochemical information from chiro-optical measurements; however, their inherent difficulty has been compounded by the fact that essentially all laboratory data available for comparison purposes stem from solution-phase studies that are subject to significant and, as of yet, poorly understood solute−solvent perturbations.[20,29]

The present work strives to alleviate environmental complexities by performing measurements of nonresonant optical activity

---

* Corresponding author. E-mail: patrick.vaccaro@yale.edu. Telephone/fax: (203) 432−3975/(203) 432−6144.
† Yale University.
‡ Gaussian, Inc.

Optical Activity in the Vapor Phase

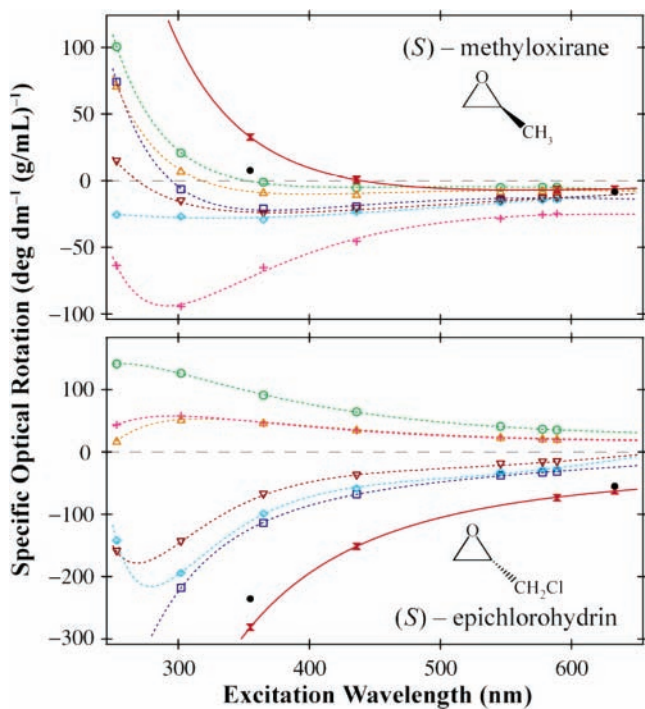*J. Phys. Chem. A, Vol. 109, No. 51, 2005* **11753**

Figure 1. Nonresonant optical activity in model chiral systems. Optical rotary dispersion (ORD) curves, showing the dependence of specific optical rotation on excitation wavelength, are plotted for two model organic compounds, (*S*)-methyloxirane and (*S*)-epichlorohydrin. The depicted results follow from canonical liquid-phase polarimetric studies performed on a variety of dilute solutions (dashed curves and opened symbols: cyclohexane (□); carbon tetrachloride (◇); di-*n*-butyl ether (▽); ethanol (△); benzene (+); and acetonitrile (○)), as well as from corresponding density functional calculations (solid red curves and hourglass symbols) and from analogous CRDP vapor-phase measurements (●). The first electronic absorption bands for the targeted species appear well below 200 nm, highlighting the nonresonant nature of the observed chiro-optical response.

under solvent-free (gas-phase) conditions, thereby lifting the veil of solvation and revealing the chiro-optical response evoked from isolated molecules. This task has been made possible by our development of cavity ring-down polarimetry (CRDP),[38,39] an ultrasensitive polarimetric scheme designed to interrogate both CB and CD phenomena in rarefied media. In brief, CRDP builds upon the exquisite detection capabilities afforded by long-path-length cavity ring-down spectroscopy (CRDS),[40] as augmented through incorporation of polarization-selective components into the light injection stage, stable resonator assembly, and signal detection train of a conventional (pulsed) CRDS apparatus. Direct comparison of the resulting vapor-phase optical activity parameters with their solution-phase and ab initio counterparts can afford a trenchant glimpse of the pronounced and, oftentimes, counterintuitive effects incurred by nonspecific solute−solvent interactions.

The investigation of optical activity in condensed media has enjoyed a long and fruitful history,[10] serving to elucidate many of the key features that distinguish the structure and dynamics of chiral molecules. The underlying motivation for our attempt to extend these efforts to the vapor phase is demonstrated succinctly by Figure 1, which presents optical rotatory dispersion (ORD) data obtained by monitoring nonresonant CB as a function of excitation wavelength for two model organic compounds, (*S*)-methyloxirane and (*S*)-epichlorohydrin. Specific optical rotation, $[\alpha]_\lambda^T$, expressing the angle of linear polarization rotation (deg) recorded at temperature T and wavelength λ per path length (dm) and per concentration (g/mL), has been

plotted on the ordinate scale. The dashed curves follow from the interpolation of canonical solution-phase polarimetric measurements performed at discrete excitation frequencies (ν) denoted by the individual symbols, with concentrations being kept low enough to minimize solute−solute interactions.[41] The selected solvent species span a wide range of chemical and physical characteristics, including permanent electric dipole moments μ, dielectric constant $\epsilon(\nu)$, and refractive indices $n(\nu) \approx \epsilon(\nu)^{1/2}$. Even a cursory inspection of Figure 1 reveals marked differences among the solution-phase results, reflecting the substantial influence of solvation and showing that the observed quantity is not an intrinsic property of the isolated solute molecule. This anomalous behavior is made more evident by the fact that all traces have been "corrected" for local field effects through use of the well-known Lorentz factor,[10,16] $\gamma_s(\nu) = (\epsilon(\nu) + 1)/3 \approx (n(\nu)^2 + 1)/3$, which stems from a rudimentary continuum-dielectric model that often has been invoked (with some trepidation[19,20]) to account for the nonspecific influence of solvation upon chiro-optical response. Clearly, analogous studies conducted in a solvent-free (gaseous) environment are essential for the reliable extraction of unperturbed (or intrinsic) molecular properties.

II. Experimental Procedures

The basic CRDP apparatus and accompanying alignment procedures employed for the present investigations of gas-phase optical activity (at nonresonant excitation wavelengths of 355 and 633 nm) were similar to those reported previously;[38,39] however, a brief description of the most salient features will prove useful for the ensuing discussion. Tunable light in the visible/ultraviolet region of the spectrum was obtained by pumping a high-resolution pulsed dye laser (Lambda Physik FL3002E; 0.035 cm^{-1} bandwidth) with the second harmonic of an injection-seeded Nd:YAG system (Spectra Physics GCR-4-20; 20 pps repetition rate; ≤10 ns pulse duration). While the fundamental dye laser output was utilized for 633 nm work, studies performed at 355 nm necessitated that it be frequency doubled (INRAD Autotracker III; BBO crystal) with the generated ultraviolet being isolated by a set of four Brewster angle prisms. The resulting light beam propagated through a variable attenuator before entering a Keplerian telescope where it was spatially filtered and refocused to match the mode structure of a ring-down cavity having a measured length of $L = 149.355(79)$ cm (one standard deviation uncertainty in the final two significant digits).

The mode-matched CRDP excitation beam (∼8 ns pulse duration; 3−5 μJ pulse energy) passed through a circular polarizer composed of a tandem calcite prism (linear polarizer) and quarter-wave plate (λ/4-retarder) prior to entering the linear resonator assembly though the planar rear surface of one cavity mirror. The mirrors employed for 355 nm and 633 nm studies (Research Electro-Optics) possessed reflectivities of $R \geq 99.95\%$ and $R \geq 99.99\%$, respectively, with the attendant radii of curvature for the substrates being 1 and 1.5 m. Two intracavity zero-order λ/4-retarders having superior antireflection coatings (Alpine Research Optics; $R < 0.15\%$ per surface) were located $d = 15.489(30)$ cm from each mirror face so as to correct for the inversion of light helicity incurred by retroreflection.[38,39] Careful alignment of these components allowed a stable, linearly-polarized field to be established in the central $l = L - 2d = 118.375(98)$ cm portion of the apparatus, thereby making this region (of fractional length $f = l/L = 0.79257(78)$) sensitive to the accruing effects of natural optical activity imposed by the introduction of chiral vapors. All experimental

data were acquired through use of the phase-sensitive or modulated mode of CRDP operation[39] whereby mechanical adjustment of the intracavity retarders imposes a polarization oscillation of known frequency upon the exponentially decaying temporal profiles of the evacuated ring-down apparatus.

Light emerging from the high-finesse resonator assembly was analyzed by utilizing a tandem quarter waveplate and calcite prism to project it onto two orthogonal axes of linear polarization, nominally representing polarization states parallel and perpendicular to that injected initially into the active cavity region of length *l*. The polarization-resolved photons impinged upon the photocathodes of matched photomultiplier tubes with the resulting pair of electrical signals, reflecting the intensities $I_\parallel$ and $I_\perp$, being directed into separate channels of a digital oscilloscope (Tektronix TDS684B; 1 GHz bandwidth, 5GS/s sampling rate) where they were averaged over 4000 laser pulses prior to being transferred to a personal computer for further processing. Reduction of the intrinsic oscilloscope bandwidth to 20 MHz by means of an internal electronic filter provided an effective means for suppressing mode-beating features superimposed on the exponentially decaying and polarization-oscillating temporal profiles.

Most of the chiral compounds examined during the present study were obtained commercially (Sigma-Aldrich); however, the lack of viable sources for (*R*)-propylenesulfide,[42] (*S*)-2-chloropropionitrile,[43] (*R*)-2-chlorobutane,[44] and (*R*)-3-chloro-1-butene[45] required that they be synthesized in-house according to procedures described in the published literature. Tables 1−3 provide a synopsis of targeted species, partitioning them into families of structurally related terpenes, epoxides, and alkanes/alkenes. Although the accompanying information regarding chemical and enantiomeric purities usually was taken from the specifications of the manufacturer, these data were corroborated by measuring the specific optical rotation for the neat liquid with sodium D-line excitation ($[\alpha]_D^{25°C}$). The purities of (*R*)-3-chloro-1-butene and (*R*)-2-chlorobutane were determined directly through use of chiral gas chromatography while that of (*S*)-2-chloropropionitrile was obtained by converting to the amide and comparing the attendant $[\alpha]_D^{25°C}$ value to that reported for samples of known enantiomeric excess.[43]

To minimize potential sources of contamination, each chiral compound was subjected to at least three freeze−pump−thaw cycles prior to having its vapor introduced into the CRDP apparatus (which had been evacuated to $\leq 10^{-6}$ Torr by means of a baffled, diffusion-pumped vacuum system). Sample pressures were maintained at constant values spanning the range of 0.3−100 Torr as measured by factory-calibrated capacitance manometers (MKS Baratron). The resulting gas-phase measurements of nonresonant optical activity were compared with analogous solution-phase results obtained through use of a commercial polarimeter (Perkin-Elmer 341; 1 dm sample path length) operating at discrete excitation wavelengths filtered from NaI and HgI atomic emission lamps. Solvents employed for the latter work were of spectrophotometric grade (Sigma-Aldrich), except for ethanol (ACS grade; 200 proof) and carbon tetrachloride (ACS reagent grade; 99.9%). Theoretical predictions of structural parameters and chiro-optical properties for all targeted molecules were obtained through use of the Gaussian03 ab initio program.[46]

III. Experimental Results

The unique capabilities afforded by CRDP for the interrogation of optical activity in rarefied media are demonstrated explicitly by Figure 2, which highlights CB measurements performed on gaseous epichlorohydrin at the nonresonant
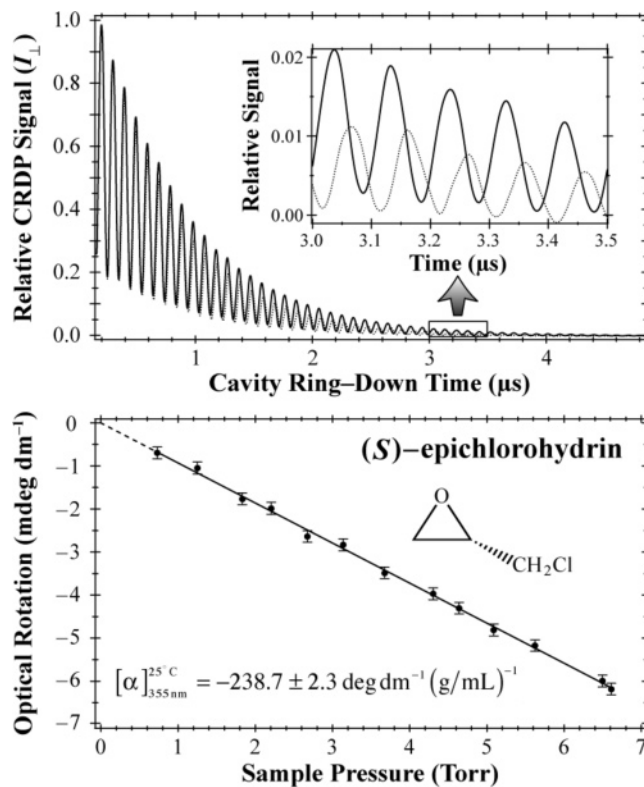

Figure 2. Demonstration of nonresonant optical activity measurement by CRDP. In the top panel, the relative intensity of 355 nm light transmitted through a ring-down polarimeter is plotted as a function of time relative to the instant of pulsed laser excitation. These data were acquired in the modulated mode of operation by monitoring the perpendicular detection channel, with signal traces displayed for an empty apparatus (solid curve) and for one containing 6.610 Torr of ambient (*S*)-epichlorohydrin vapor (dotted curve). As highlighted by the inset, the action of natural optical activity leads to a marked shift in the oscillation frequency from which the chiro-optical response of the sample can be extracted. The bottom panel shows the dependence of measured 355 nm polarization rotation per unit path length, ϕ, on epichlorohydrin pressure, p. The linear scaling with number density and accompanying zero intercept confirm the isolated nature of the targeted species. Least-squares regression yields a slope of $d\phi/dp = -9.420 \pm 0.090$ mdeg dm^{-1} Torr^{-1} which corresponds to a specific rotation of $[\alpha]_{355nm}^{25°C} = -238.7 \pm 2.3$ deg dm^{-1} (g/mL)$^{-1}$ (one standard deviation uncertainties).

excitation wavelength of 355 nm. The top panel depicts ring-down traces obtained by monitoring the perpendicular detection channel (i.e., $I_\perp$) as a function of time (referenced to the instant that the incident light pulse first enters the cavity). Results are presented both for an evacuated polarimeter (solid curve) and for one containing a $p = 6.610$ Torr sample of ambient (*S*)-epichlorohydrin vapor (dotted curve). These data sets were acquired sequentially through use of the phase-sensitive or modulated mode of operation,[39] with the polarization oscillation frequency imposed upon the exponentially decaying profile of the empty apparatus, ω_0', being determined by mechanical adjustment of the intracavity $\lambda/4$-retardation plates. In particular, ω_0' (or ω_p' for $p \neq 0$) describes the rate of linear polarization rotation (in units of angle/time or, equivalently, angle/length) as light repeatedly traverses the optical resonator assembly. The signals emerging from the parallel detection channel (i.e., $I_\parallel$) were recorded simultaneously and found to be similar in shape to their $I_\perp$ counterparts, exhibiting oscillations of identical frequency but of quadrature phase.

The introduction of a chiral vapor into the CRDP apparatus produces a change in the rate of polarization modulation as the

Optical Activity in the Vapor Phase

J. Phys. Chem. A, Vol. 109, No. 51, 2005 **11755**

action of natural optical activity either increases or decreases ω'_p relative to that of the evacuated instrument,[38,39] with the sign of the observed frequency shift depending on the enantiomeric form of the entrained species. While the resulting frequency difference, $\Delta\omega'_p = \omega'_p - \omega'_0$, is expected to be minute in magnitude, the enormous effective path length realized by having light undergo multiple reflections in a high-finesse resonator assembly greatly enhances the manifestation of such effects. This is demonstrated clearly by the top panel of Figure 2 where the inset presents an expanded view of the diverging temporal behavior exhibited by the two $I_\perp$ traces (for empty and filled polarimeters) in the vicinity of 3 μs which corresponds to a sample path length in excess of 1 km. As discussed below, the measured value of $\Delta\omega'_p$ can be converted readily into the angle of linear polarization rotation accrued per unit distance, ϕ, which, in turn, can be combined with the known density of target molecules to yield the specific optical rotation at excitation wavelength λ, $[\alpha]^T_\lambda$.

The quantitative extraction of optical activity information from temporal data sets such as those depicted in the top panel of Figure 2 builds upon our previously reported theoretical analyses of the CRDP methodology.[39] In brief, this treatment relies upon a matrix representation of polarization state[47] to describe the changes in transverse characteristics accrued as a beam of light undergoes N round-trip passes through the linear resonator assembly (of length L) that forms the heart of the apparatus. It proves convenient to consider the radiation introduced initially into the active region of the polarimeter (of length $l = L - 2d$) to be polarized completely, but not in a strictly linear sense, such that the amplitude-normalized polarization vector for the injected electromagnetic field has the form[39,47]

$$\mathbf{P}_i = \frac{\sqrt{b}}{2}\left[\left(1 + \sqrt{\frac{2-b}{b}}\right)\hat{\mathbf{e}}_\parallel - i\left(1 - \sqrt{\frac{2-b}{b}}\right)\hat{\mathbf{e}}_\perp\right] \quad (1)$$

where $\hat{\mathbf{e}}_\parallel$ and $\hat{\mathbf{e}}_\perp$ denote orthogonal unit vectors that span the plane transverse to the direction of collimated beam propagation. The parameter b ($0 \le b \le 2$) adjusts the polarization state of the attendant wave from right circular ($b = 0$) through linear ($b = 1$ where $\mathbf{P}_i = \hat{\mathbf{e}}_\parallel$) and onto left circular ($b = 2$). For b close to unity, $\mathbf{P}_i$ describes an injected electromagnetic field that is polarized elliptically with its major axis aligned along the direction specified by $\hat{\mathbf{e}}_\parallel$. This situation is reminiscent of that encountered when a linearly polarized beam of light passes though a transparent, yet slightly birefringent, medium (e.g., a cavity mirror substrate).[39]

Given the expression for $\mathbf{P}_i$ in eq 1 and assuming that the excitation wavelength is removed sufficiently from resonance such that CD phenomena justifiably can be neglected ($\Delta\epsilon = \epsilon_L - \epsilon_R = 0$), the intensities recorded on the parallel and perpendicular detection channels of the CRDP apparatus are predicted to have the forms[39]

$$I_\parallel = R^{2N}e^{-\epsilon L(2N+1)}\left\{\frac{1 - \sqrt{b(2-b)}}{2} + \sqrt{b(2-b)}\cos^2[(2N+1)(\alpha+\phi l)]\right\} \quad (2)$$

$$I_\perp = R^{2N}e^{-\epsilon L(2N+1)}\left\{\frac{1 - \sqrt{b(2-b)}}{2} + \sqrt{b(2-b)}\sin^2[(2N+1)(\alpha+\phi l)]\right\} \quad (3)$$

where $\epsilon = (\epsilon_L + \epsilon_R)/2$ and $\phi = \pi\Delta n/\lambda$ denote the total absorption/scattering (or net attenuation) per unit path length and optical activity (or polarization rotation) per unit path length, respectively, while α represents the complement of the displacement angle established between the fast axes of the two intracavity waveplates. It is important to recognize that ϕ (as well as ϵ) should scale linearly with target number density and drop to zero in the limit of an evacuated apparatus. In contrast, the value of α is fixed by mechanical alignment of the $\lambda/4$-retarders within the polarimeter body and should remain constant independent of the sample pressure. The quantity R ($0 \le R \le 1$) appearing in eqs 2 and 3 defines the effective reflectivity for each mirror in the resonator, embodying the efficiency of the mirror coating as well as the inevitable losses introduced by the adjacent intracavity waveplate.

Since N is related to the round-trip period of an optical pulse trapped in the resonator assembly, $t_{rt} = 2L/c$, it follows that $I_\parallel$ and $I_\perp$ can be recast as functions of time. The resulting exponentially decaying temporal profiles are predicted[39] to oscillate at a common frequency determined by the combined effects of α and ϕl, which collectively govern the rotation of polarization taking place in the active region of the polarimeter. Complications arising from polarization imperfections[39] (e.g., $b \ne 1$ in eq 1) can be mitigated by subtracting $I_\perp$ from $I_\parallel$, with the quadrature relationship between the polarization modulations superimposed on these concurrently recorded traces leading to

$$I_\parallel - I_\perp = \sqrt{b(2-b)}e^{-\epsilon L(2N+1)}R^{2N}\cos[2(2N+1)(\alpha+\phi l)]$$
$$= A_p e^{-\Gamma_p t}\cos[\omega_p t + \Phi_p] \quad (4)$$

where $A_p = \sqrt{b(2-b)}\ e^{-\epsilon L}$, $\Gamma_p = c(|\ln R| + \epsilon L)/L$, $\omega_p = 2c(\alpha + \phi l)/L$, and $\Phi_p = 2(\alpha + \phi l)$ denote the amplitude, decay rate, angular modulation frequency (with $\omega_p = 2\omega'_p$), and relative phase factor, respectively, for the $I_\parallel - I_\perp$ difference signal. The subscript of "p" affixed to each of these quantities emphasizes that they should depend on the pressure of chiral vapor introduced into the CRDP apparatus. The transformation of variables embodied in the second equality of eq 4 has exploited the fact that $t = Nt_{rt} = 2NL/c$ in order to convert between the number of round-trip passes (N) and the ring-down time (t).[39]
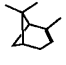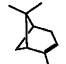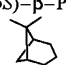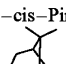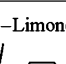
The time-domain difference signal defined by eq 4 closely resembles that of an idealized free-induction decay (FID), as often encountered in the realm of magnetic resonance spectroscopy.[48] Consequently, Fourier transformation with minimal zero-padding ($2-4\times$) was used to obtain the frequency-domain $I_\parallel - I_\perp$ power spectrum for a simultaneously recorded pair of $I_\parallel$ and $I_\perp$ traces, with subsequent nonlinear least-squares regression based upon a Lorentzian line shape model allowing for quantitative extraction of the angular modulation frequency ω_p. In particular, the desired chiro-optical response of the gaseous target medium can be isolated from $\omega_p = 2c(\alpha + \phi l)/L$ by examining the change in this quantity, $\Delta\omega_p$, between a filled (at pressure $p \ne 0$) and evacuated (at pressure $p = 0$) polarimeter:

$$\Delta\omega_p = \omega_p - \omega_0 = 2c\left(\frac{l}{L}\right)\phi = 2cf\phi \quad (5)$$

where $f = l/L$ denotes the fraction of the cavity length that is sensitive to optical activity (the active fraction) and ω_0 signifies the value of ω_p for $p = 0$.

The lower panel in Figure 2 illustrates the pressure dependence for the angle of linear polarization rotation per unit path

TABLE 1: Specific Optical Rotation of Model Terpene Compounds[a]

Optically-Active Sample	Purity and Density (g/mL)	Excitation Wavelength (nm)	Measured Gas-Phase Specific Rotation	Extrapolated Solution-Phase Specific Rotation	Calculated Specific Rotation for Isolated Molecule	
					B3LYP (pVDZ)	B3LYP (pVTZ)
(1R, 5R)−α−Pinene	≥ 99% (97% ee) $[\alpha]_D^{25°C} = 49.93$ $d = 0.856$	355	188.2 ± 2.2	171.2	102.6	104.7
		633	46.3 ± 2.5	43.4	38.5	38.0
(1S, 5S)−α−Pinene	99% (97% ee) $[\alpha]_D^{25°C} = -50.65$ $d = 0.856$	355	−187.0 ± 2.4	−171.2	−102.6	−104.7
		633	−46.0 ± 2.5	−43.4	−38.5	−38.0
(1S, 5S)−β−Pinene	≥ 99% (97% ee) $[\alpha]_D^{25°C} = -21.59$ $d = 0.866$	355	69.7 ± 3.2	24.7	260.6	...
		633	−4.66 ± 0.60	−18.3	21.3	...
(1R)−cis−Pinane	99% $[\alpha]_D^{25°C} = 23.68$ $d = 0.856$	355	61.9 ± 3.5	82.8	71.0	...
		633	12.2 ± 2.6	18.1	15.8	...
(R)−Limonene	97% (98% ee) $[\alpha]_D^{25°C} = 122.80$ $d = 0.840$	355	315.5 ± 7.4	407.1	270.3	...
		633	62.1 ± 7.1	100.1	76.3	...

[a] Specific optical rotation ($[\alpha]_\lambda^{25°C}$) is tabulated in the units of deg dm^{-1} (g/mL)$^{-1}$ for a variety of organic compounds belonging to the terpene family. The chemical and enantiomeric purities of each chiral sample are indicated, as are the corresponding values of $[\alpha]_D^{25°C}$ (sodium D-line excitation) and density (d, in g/mL) for the neat liquid. Gas-phase CRDP measurements were performed under ambient conditions through direct 355 and 633 nm laser excitation, while analogous solution-phase data were extrapolated from discrete-wavelength polarimetric studies conducted in dilute cyclohexane media. Predicted specific rotation values for isolated (solvent-free) molecules follow from linear response calculations carried out by means of B3LYP/aug-cc-PVDZ and B3LYP/aug-cc-PVTZ density functional methods. The ab initio results for α-pinene, β-pinene, and cis-pinane reflect properties expected for the minimum-energy configuration of the nuclear framework, with requisite geometry optimizations being done at the B3LYP/6-311+G* level of theory. Similar structural analyses of limonene revealed three low-lying conformers, which were taken into account by thermally averaging their attendant contributions to the total chiro-optical response.

length, ϕ (in mdeg dm^{-1}), extracted from 355 nm CRDP measurements of CB in ambient (S)-epichlorohydrin vapor. As expected for isolated, gas-phase species, a linear relationship is found to hold between ϕ and p, with least-squares analysis revealing a null (to within experimental uncertainty) zero-pressure intercept of $\phi_0 = -54 \pm 84$ μdeg dm^{-1}. Of special importance for the quantification of optical activity is the corresponding slope, $d\phi/dp = -0.9420(90)$ mdeg dm^{-1} Torr^{-1} (as obtained by constraining the intercept to be zero), which, upon performing the appropriate transformation between pressure (in Torr) and concentration (in g/mL) under the assumption of an ideal gas, yields a specific optical rotation value of $[\alpha]_{355nm}^{25°C} = -238.7 \pm 2.3$ deg dm^{-1} (g/mL)$^{-1}$.

To assess the overall reliability of CRDP as a probe of nonresonant optical activity in the vapor phase, pressure-dependent studies were performed in tandem on the two enantiomers of α-pinene (cf., Table 1), as well as on their corresponding racemic mixture. As highlighted by Figure 3, polarization rotation data acquired for optically pure (R)-α-pinene and (S)-α-pinene vapor gave nonzero slopes ($d\phi/dp$) of equal magnitude (to within experimental uncertainty), yet opposite sign, leading to 355 nm specific rotation parameters ($[\alpha]_{355nm}^{25°C}$) of +188.2 ± 2.2 deg dm^{-1} (g/mL)$^{-1}$ and −187.0 ± 2.4 deg dm^{-1} (g/mL)$^{-1}$, respectively. In contrast, a null value of ϕ was measured at all sample pressures in the case of racemic α-pinene. These results are in keeping with the inverse chiro-optical response predicted for the molecules comprising an enantiomeric pair and the absence of net optical activity expected for their racemic mixture.[10,11]
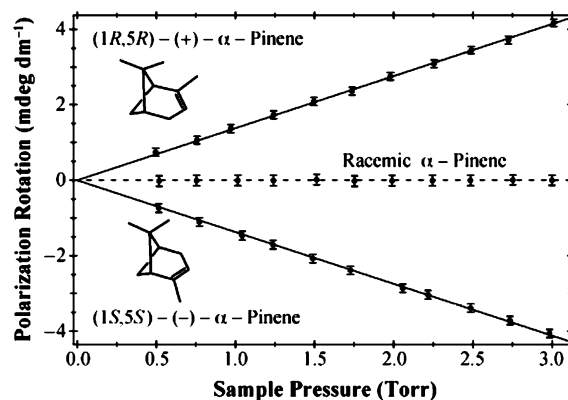

Figure 3. Pressure dependent CRDP studies on optically-pure and racemic α-pinene. The measured 355 nm optical rotation per unit path length is plotted as a function of pressure for vapor-phase samples of (R)-α-pinene, (S)-α-pinene, and racemic α-pinene. As expected, data sets acquired for the optically pure enantiomers scale linearly with number density, exhibiting nonzero slopes of equal magnitude, but opposite sign. Regression analyses yield $d\phi/dp$ values of +1.380 ± 0.016 and −1.371 ± 0.017 mdeg dm^{-1} Torr^{-1}, which correspond to specific rotations ($[\alpha]_{355nm}^{25°C}$) of +188.2 ± 2.2 and −187.0 ± 2.4 deg dm^{-1} (g/mL)$^{-1}$ for the (R) and (S) forms, respectively (one standard deviation uncertainties). The null value of ϕ obtained at all sample pressures for the racemic α-pinene mixture is in keeping with the anticipated absence of net optical activity.

Given the substantial electromagnetic field strengths available from pulsed laser sources, it is interesting to speculate on the possible roles that higher-order interactions[9,49] may play for the

Optical Activity in the Vapor Phase

J. Phys. Chem. A, Vol. 109, No. 51, 2005 **11757**

interrogation of optical activity by (laser-based) CRDP techniques. While resonant two-photon CD has been explored extensively,[9,50] theoretical predictions[51] for the existence of analogous nonlinear or multiphoton CB phenomena have been corroborated by only a handful of solution-phase studies.[52,53] In particular, Cameron and Tabisz[53] employed strongly focused 308 nm radiation from a nanosecond-duration excimer laser to demonstrate that extracted specific rotation parameters, $[\alpha]_{308nm}^T$, could be decomposed into contributions arising from simultaneous one-photon, $[\alpha^{(1)}]_{308nm}^T$, and two-photon, $[\alpha^{(2)}]_{308nm}^T$, processes. Experiments conducted on aqueous uridine and sucrose solutions (∼0.2 M) at fluences of ∼27.8 J/cm² gave $[\alpha^{(2)}]_{308nm}^T/[\alpha^{(1)}]_{308nm}^T$ ratios of -1.8×10^{-3} and -5.5×10^{-4}, respectively, with the magnitude of $[\alpha^{(2)}]_{308nm}^T$ found to scale quadratically as a function of laser power. Such conditions are to be contrasted with those utilized for the present CRDP work, where the minute fraction of excitation light that passes through the resonator input mirror $(1 - R \le 5 \times 10^{-4})$ leads to intracavity fluences of less than 7×10^{-7} J/cm² (assuming an intracavity beam waist of 0.03 cm). This represents nearly 8 orders of magnitude reduction in optical energy relative to that needed by prior two-photon CB investigations and would tend to discount significant influence of higher-order nonlinear/multiphoton effects, an assertion supported by the lack of any discernible intensity dependence in our gas-phase measurements of chiro-optical properties.

Tables 1−3 present a summary of specific optical rotation parameters determined at the two available CRDP excitation wavelengths of 355 and 633 nm under ambient (25 °C), bulk-gas conditions. These quantities are meant to augment and supersede those emerging from our prior work,[38,39] with the use of pressure-dependent analyses (cf., Figure 2) rather than the averaging of many data sets acquired at comparable pressures (as previously employed) thought to enhance substantially the overall accuracy of extracted $[\alpha]_\lambda^T$ values. Indeed, the accompanying one standard deviation uncertainties, obtained through conventional propagation of error techniques, are found to be in excellent accord with the reproducibility gauged by repeating CRDP experiments at different times. Aside from pertinent information regarding the purity of targeted chiral samples, Tables 1−3 also contain ab initio predictions for the nonresonant optical activity of isolated (solvent-free) molecules as well as analogous condensed-phase $[\alpha]_{355nm}^{25°C}$ and $[\alpha]_{633nm}^{25°C}$ parameters interpolated from discrete-wavelength polarimetric studies performed on dilute (<0.1 M) cyclohexane solutions. The tabulated theoretical results reflect properties calculated for the optimized (minimum-energy) geometry of each molecular framework, with the flexibility inherent to nonrigid species (e.g., limonene, epichlorohydrin, etc.) leading to several low-lying conformers that often display antagonistic chiro-optical behavior. As discussed below, proper treatment of such systems demands use of statistical averaging procedures to account for the thermal population of multiple structural isomers.
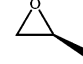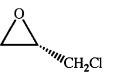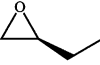
IV. Discussion

Figure 1 highlights the dual role that the chiro-optical response of an isolated molecule can play for elucidating the origin of solvent effects and assessing the reliability of theoretical calculations. The filled circular symbols appearing in this figure follow from pressure-dependent CRDP measurements of gas-phase optical activity performed at the nonresonant excitation wavelengths of 355 and 633 nm. While the ground electronic potential surface of methyloxirane (top panel) supports a rigid

equilibrium geometry with a 3-fold barrier to methyl rotation of 2.7 kcal/mol height,[54] the more flexible nature of epichlorohydrin (bottom panel) leads to several low-lying structures of similar energy (vide infra). The 633 nm results for isolated and solvated (S)-methyloxirane are in good accord (excluding the case of benzene solvent); however, a substantial discrepancy is present at 355 nm where $[\alpha]_{355nm}^{25°C}$ apparently changes sign as the surrounding solvent molecules are "removed" from the chiral solute.[55] As discussed below, much less satisfactory agreement is found for (S)-epichlorohydrin, reflecting the differential stabilization of solvated conformers each of which contributes uniquely to the total specific rotation.[41,56,57] It should be noted that a handful of attempts to observe polarization rotation in chiral vapors have been documented since the discovery of chiro-optical phenomena nearly two centuries ago;[58] however, our CRDP work surprisingly represents the first quantitative extraction of such information under ambient conditions.

Nonresonant CB imposes unique challenges for quantum chemistry calculations since this composite electric/magnetic property reflects dynamical response of the *entire* electronic distribution to oscillating electromagnetic fields (rather than depending primarily on the electronic provenance of a localized chromophore as often is the case for resonant CD). Nevertheless, recent years have witnessed the rapid development of coupled cluster[59] (CC) and density functional theory[60,61] (DFT) techniques designed specifically for the ab initio prediction of ORD profiles. Owing to its accurate incorporation of electron-correlation effects (essential for the quantitative description of electric and magnetic interactions), CC long has been recognized to provide the superior theoretical framework;[62] however, the substantially greater computational efficiency afforded by DFT methods has led to their dominance in studies of chiro-optical phenomena.[14,17−21,23,24,28,36,63] Successful application of the requisite time-dependent density functional formalism[61] (TD-DFT) demands use of large basis sets that include diffuse functions on all nuclei,[18,64] with the introduction of gauge-invariant atomic orbitals[27,65] (GIAOs or London orbitals) yielding $[\alpha]_\lambda^T$ values that are independent of coordinate origin (magnetic properties generally depend on the gauge origin selected for the vector potential[66]) and converge rapidly to the hypothetical complete basis-set limit (since GIAOs respond correctly to magnetic fields through first order[67]). Recent TDDFT/GIAO analyses conducted on a series of rigid chiral compounds have suggested that the average discrepancy attained for specific rotation calculations at the sodium D-line (as gauged by comparing isolated-molecule predictions with solution-phase measurements) to be $\pm 25 - 35$ deg dm⁻¹(g/mL)⁻¹.[19,21]

The hourglass symbols and solid curves in Figure 1 denote nonresonant optical activity predictions made for isolated (S)-methyloxirane and (S)-epichlorohydrin molecules by means of substantial B3LYP/aug-cc-pVTZ and B3LYP/aug-cc-pVDZ density functional treatments, with requisite equilibrium geometries being optimized at comparable MP2 levels of theory (MP2 often gives more reliable predictions of equilibrium structures than DFT).[68] As discussed in detail below, three low-lying conformers were identified for epichlorohydrin and accounted for by thermally averaging the corresponding specific rotation parameters at each excitation wavelength. While these computational results mimic the CRDP gas-phase behavior, discrepancies between experiment and theory appear to increase as the incident light frequency approaches electronic resonance (occurring at $\lambda < 200$ nm). Analogous conclusions can be gleaned from the TDDFT/GIAO predictions compiled in Tables 1−3 for all of the chiral species targeted during the present

TABLE 2: Specific Optical Rotation of Model Epoxide Compounds[a]

Optically-Active Sample	Purity and Density (g/mL)	Excitation Wavelength (nm)	Measured Gas-Phase Specific Rotation	Extrapolated Solution-Phase Specific Rotation	Calculated Specific Rotation for Isolated Molecule	
					B3LYP (pVDZ)	B3LYP (pVTZ)
(S)−Methyloxirane	99.9% $[\alpha]_D^{25°C} = -13.93$ $d = 0.829$	355	7.49 ± 0.30	−25.0	2.5	21.3
		633	-8.39 ± 0.20	−14.3	−16.2	−9.9
(S)−Epichlorohydrin	98% (97% ee) $[\alpha]_D^{25°C} = 41.94$ $d = 1.183$	355	-238.7 ± 2.3	−167.7	−260.8	...
		633	-55.0 ± 1.7	−30.4	−56.8	...
(S)−1,2−Epoxybutane	98% $[\alpha]_D^{25°C} = -9.73$ $d = 0.837$	355	-13.56 ± 0.95	−17.7	−19.2	−16.5
		633	-12.33 ± 0.35	−13.1	−18.8	−17.5
(R)−Methylthiirane	... $[\alpha]_D^{25°C} = 48.79$ $d = 0.946$	355	64.7 ± 2.3	63.2	−50.0	−113.7
		633	36.5 ± 1.7	26.9	47.1	25.6

[a] Specific optical rotation ($[\alpha]_\lambda^{25°C}$) is tabulated in the units of deg dm^{-1} (g/mL)$^{-1}$ for a variety of organic compounds belonging to the epoxide family. The chemical and enantiomeric purities of each chiral sample are indicated, as are the corresponding values of $[\alpha]_D^{25°C}$ (sodium D-line excitation) and density (d, in g/mL) for the neat liquid. Gas-phase CRDP measurements were performed under ambient conditions through direct 355 and 633 nm laser excitation, while analogous solution-phase data were extrapolated from discrete-wavelength polarimetric studies conducted in dilute cyclohexane media. Predicted specific rotation values for isolated (solvent-free) molecules follow from linear response calculations carried out by means of B3LYP/aug-cc-PVDZ and B3LYP/aug-cc-PVTZ density functional methods. The ab initio results for methyloxirane and methylthiirane reflect properties expected for the minimum-energy configuration of the nuclear framework, with requisite geometry optimizations being done at the MP2/6-311++G** level of theory. Similar MP2/6-311+G* analyses of epichlorohydrin and epoxybutane revealed three low-lying conformers, which were taken into account by thermally averaging their attendant contributions to the total chiro-optical response. It is interesting to note that $[\alpha]_D^{25°C}$ for neat (S)-epichlorohydrin is positive while analogous quantities measured under either (isolated) gas-phase or (dilute) solution-phase conditions have the opposite sign.

investigation. The nominally rigid terpene family (cf., Table 1) affords an especially insightful example of this phenomenon, showing that removal of the $C{=}C$ chromophore from α-pinene to obtain the structurally related *cis*-pinane system (which has its electronic transitions shifted to much higher energies) leads to vastly improved 355 nm predictions for chiro-optical behavior. In contrast, ab initio calculations performed on β-pinene (which differs from α-pinene only in the location of the $C = C$ moiety) fail to duplicate the zero-crossing found in both solution-phase and vapor-phase ORD data, thereby giving the incorrect sign for $[\alpha]_{633nm}^{25°C}$ and a value of $[\alpha]_{355nm}^{25°C}$ that is much too large in magnitude. On a similar note, recent high-level CC analyses[31,33] have questioned the ability of TDDFT to correctly reproduce the change in $[\alpha]_{355nm}^{25°C}$ sign that accompanies "removal" of solvent molecules from an (S)-methyloxirane solute[24,31,34] (cf., Figure 1 and Table 2), suggesting that such findings stem from a fortuitous cancellation of errors inherent to the density functional scheme.
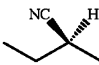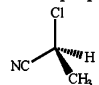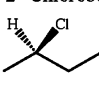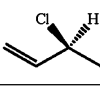
Detailed comparison of the complementary vapor-phase and solution-phase ORD data in each panel of Figure 1 reveals pronounced differences between chiro-optical properties measured for the targeted epoxide systems. While solvents possessing high static dielectric constants (e.g., acetonitrile where $\epsilon = 36.6$) are found to best mimic the isolated-molecule behavior evoked from (S)-methyloxirane and other rigid chiral species (vide infra), the opposite trend appears to hold in the case of (S)-epichlorohydrin. As suggested by previous polarimetric studies,[41,57] this disparity can be traced to the conformational flexibility of epichlorohydrin,[56] which gives rise to several low-lying structural isomers that antagonistically contribute to the total optical activity.

Table 4 contains a summary of optimized structural parameters, electric dipole moment magnitudes, and relative energies calculated for the three lowest-lying conformers of (S)-epichlorohydrin at the MP2/6-311++G** level of theory. As illustrated by the accompanying Newman projections, the global energy minimum for an isolated epichlorohydrin molecule, designated as the *gauche* II form, has the chlorine atom displaced essentially as far as possible from the oxygen center of the epoxide ring. Owing to increased steric repulsion, the remaining *gauche* I and cis configurations are predicted to reside 0.55 and 1.50 kcal/mol, respectively, above their *gauche* II counterpart. Consequently, a thermally equilibrated ensemble of gaseous epichlorohydrin will be a mixture of *gauche* II (0.634), *gauche* I (0.270), and cis (0.047) species, where the values in parentheses denote the fractional populations expected under ambient (25 °C) conditions. By excluding vibrationally mediated isomerization and tunneling processes, the computation of nonresonant optical activity at a given wavelength (λ) and temperature (T) now must be expressed as a weighted average taken over the specific rotation of each participating conformer, $[\alpha]_{\lambda,i}^T$:

$$[\alpha]_\lambda^T = \sum_i^{conformers} c_i \, [\alpha]_{\lambda,i}^T \qquad (6)$$
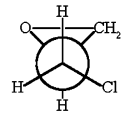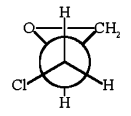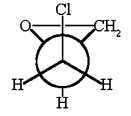
where the fractional population coefficients, $\{c_i\}$, implicitly depend on sample temperature. Table 5 presents a compilation of nonresonant optical activity parameters calculated for the low-lying conformers of (S)-epichlorohydrin at the B3LYP/aug-cc-pVDZ level of theory. For each excitation wavelength examined, the chiro-optical response for the *gauche* I species is found to be of opposite polarity to that for either the *gauche* II or cis

Optical Activity in the Vapor Phase

J. Phys. Chem. A, Vol. 109, No. 51, 2005 **11759**

TABLE 3: Specific Optical Rotation of Model Alkane and Alkene Compounds[a]

Optically-Active Sample	Purity and Density (g/mL)	Excitation Wavelength (nm)	Measured Gas-Phase Specific Rotation	Extrapolated Solution-Phase Specific Rotation	Calculated Specific Rotation for Isolated Molecule	
					B3LYP (pVDZ)	B3LYP (pVTZ)
(S)−2−Methylbutyronitrile	98% (99% ee) $[\alpha]_D^{25°C} = 36.3$ $d = 0.786$	355	136.7 ± 4.0	110.1	152.3	146.9
		633	35.4 ± 2.3	29.0	39.9	38.8
(S)−2−Chloropropionitrile	(93% ee) $[\alpha]_D^{25°C} = -14.5$ $d = 1.02$	355	−37.9 ± 2.9	−64.1	−60.6	−73.3
		633	−6.8 ± 2.3	−13.7	−12.7	−16.1
(R)−2−Chlorobutane	(93.2% ee) $[\alpha]_D^{25°C} = -31.5$ $d = 0.873$	355	−121.4 ± 1.2	−111.5	−127.8	−121.3
		633	−32.3 ± 1.0	−28.6	−33.8	−31.8
(S)−3−Chloro−1−Butene	(47.1% ee) $[\alpha]_D^{25°C} = 51.6$ $d = 0.900$	355	259.4 ± 1.0	233.1	491.5	493.7
		633	53.3 ± 1.0	45.3	90.0	89.0

[a] Specific optical rotation ($[\alpha]_\lambda^{25°C}$), *corrected for enantiomeric excess*, is tabulated in the units of deg dm^{-1} (g/mL)$^{-1}$ for a variety of organic compounds belonging to the alkane and alkene families. The chemical and enantiomeric purities of each chiral sample are indicated, as are the corresponding values of $[\alpha]_D^{25°C}$ (sodium D-line excitation) and density (*d*, in g/mL) for the neat liquid. Gas-phase CRDP measurements were performed under ambient conditions through direct 355 and 633 nm laser excitation, while analogous solution-phase data were extrapolated from discrete-wavelength polarimetric studies conducted in dilute cyclohexane media. Predicted specific rotation values for isolated (solvent-free) molecules follow from linear response calculations carried out by means of B3LYP/aug-cc-PVDZ and B3LYP/aug-cc-PVTZ density functional methods. The ab initio results for 2-chloropropionitrile reflect properties expected for the minimum-energy configuration of the nuclear framework, with the requisite geometry optimization being done at the B3LYP/aug-cc-PVDZ level of theory. Similar structural analyses of 2-methylbutyronitrile (MP2/6-311+G*), 2-chlorobutane (MP2/6-311+G*), and 3-chloro-1-butene (CCD/6-311++G(2df,2pd)) revealed three low-lying conformers, which were taken into account by thermally averaging their attendant contributions to the total chiro-optical response.

TABLE 4: Calculated Properties for (S)-Epichlorohydrin Conformers[a]

Epichlorohydrin Conformer	O−C−C−Cl Torsion Angle	H−C−C−Cl Torsion Angle	Electric Dipole Moment μ (D)	Vapor-Phase ($\varepsilon = 1.0$)		Acetonitrile Solution ($\varepsilon = 36.6$)	
				Relative Energy (kcal/mol)	Conformer Population (%)	Relative Energy (kcal/mol)	Conformer Population (%)
Gauche II	163.2	−59.7	0.634	0.00	68.3	0.11	42.8
Gauche I	−80.5	57.1	3.432	0.55	27.0	0.00	51.5
Cis	45.7	−176.1	2.486	1.58	4.7	1.31	5.7

[a] The three lowest-lying conformers of (S)-epichlorohydrin predicted at the MP2/6-311+G* level of theory are illustrated by means of Newman projections and defined in terms of their respective torsion angles. The relative energies and Boltzmann-weighted populations (at 25 °C) for the *gauche* I, *gauche* II, and cis forms are tabulated, with use of an IPCM implicit solvation model, suggesting that their energy ordering changes between the isolated vapor ($\epsilon = 1.0$) and acetonitrile solution ($\epsilon = 36.6$) phases where values in parentheses denote the corresponding dielectric constants. This differential stabilization of conformers in solvent-mediated environments can be attributed primarily to the distinct permanent electric dipole moment (of magnitude μ in units of Debye) supported by each species.

form. This antagonistic behavior imparts a characteristic temperature dependence to the overall specific rotation, necessitating use of the averaging procedure embodied in eq 6. As shown by the ORD curves in the lower panel of Figure 1 and reinforced by the numerical data in Table 5, the conformer-weighted ab initio predictions of $[\alpha]_\lambda^T$ for isolated (S)-epichlorohydrin

molecules (with $\{c_i\}$ values determined from relative conformer energies) are in reasonable accord with the gas-phase results obtained from CRDP measurements. Similar analyses are required to account fully for the chiro-optical behavior exhibited by other nonrigid species (e.g., limonene and epoxybutane).

TABLE 5: Optical Rotation Parameters for (S)-Epichlorohydrin[a]

excitation wavelength (nm)	calculated specific optical rotation for individual conformers			predicted specific optical rotation (Boltzmann-averaged at 25 °C)		measured solution-phase specific optical rotation acetonitrile solution ($\epsilon = 36.6$)
	gauche II	*gauche* I	*cis*	vapor phase ($\epsilon = 1.0$)	acetonitrile solution ($\epsilon = 36.6$)	
633	−137.0	+143.4	−42.0	−56.8	+12.9	+37.8
589	−160.8	+166.9	−50.4	−67.1	+14.3	+44.5
436	−327.9	+335.9	−117.3	−138.7	+26.1	+82.1
355	−565.6	+505.3	−234.4	−260.8	+5.0	+123.3

[a] B3LYP/aug-cc-PVDZ linear response theory has been exploited to calculate specific optical rotation parameters (in deg dm^{-1} (g/mL)$^{-1}$) at a series of nonresonant excitation wavelengths for each of the low-lying structural isomers in (S)-epichlorohydrin. By taking into account conformer populations under ambient conditions, Boltzmann-weighted values of $[\alpha]_{\lambda}^{25°C}$ have been determined for isolated-vapor and acetonitrile-solution phases, where the latter follow from an IPCM implicit solvation model. The thermally averaged optical activity of solvent-free (S)-epichlorohydrin is predicted to change sign in a dilute acetonitrile medium, an assertion in keeping with the results obtained from polarimetric measurements.

The three low-lying conformers of epichlorohydrin are predicted to support grossly different permanent electric dipole moments (cf., Table 4), with the magnitude of this quantity for the *gauche* I form (3.432 D) greatly exceeding that for its cis (2.486 D) and *gauche* II (0.634 D) counterparts. To explore the ramifications for nonresonant optical activity in condensed media, the ab initio energy for each structural isomer was recalculated by exploiting a polarizable continuum model[20,69] (PCM) to treat nonspecific solvation phenomena in conjunction with a static isodensity surface technique[70] to generate the requisite solute cavity. For a dielectric constant selected to mimic acetonitrile ($\epsilon = 36.6$), this IPCM approach suggests significant stabilization of the more polar conformations, leading to a change in relative energy ordering that has the *gauche* I species as the global minimum (cf., solution-phase and vapor-phase energy predictions in Table 4). The attendant shifts in fractional population coefficients for a thermally equilibrated ensemble of (S)-epichlorohydrin are found to reverse the polarity of total specific rotation (relative to the isolated molecule) for all of the excitation wavelengths compiled in Table 5, reflecting, once again, the antagonistic chiro-optical response evoked from participating species. While our rudimentary analyses (which combine implicit-solvation energy estimates with vapor-phase $[\alpha]_{\lambda,i}^{T}$ predictions) fail to reproduce the detailed wavelength dependence of ORD curves recorded in dilute acetonitrile solutions, the key assertion of a sign inversion upon solvation does agree with the results of polarimetric measurements.

The surprising disparity between the nonresonant chiro-optical response evoked from isolated and solvated species is emphasized by Figure 4 which plots specific optical rotation for the nominally rigid (R)-cis-pinane system against a quantity related to the static dielectric constant, ϵ, of the surrounding medium. The depicted data follow from CRDP gas-phase (filled symbols) and canonical solution-phase (opened symbols) polarimetric studies, with the two panels distinguishing results obtained for (a) 355 nm and (b) 633 nm excitation. The abscissa for each graph is defined in terms of the Onsager dielectric function, $g(\epsilon) = (\epsilon - 1)/(2\epsilon + 1)$, which spans the range $0.0 \leq g(\epsilon) \leq 0.5$ as one moves from rarefied vapor ($\epsilon = 1.0$) to solvents of high polarity ($\epsilon \gg 1$). This analysis builds upon the well-known concepts of Onsager reaction field theory[71] where the multipole moments of a (potentially polarizable) solute molecule, imbedded in an isotropic and homogeneous continuum-dielectric solvent, induce reflection moments that, in turn, act to electrostatically stabilize the solute. In simplest form, this venerable approach encloses the solute in a spherical cavity of radius a and only considers the molecular dipole moment μ, thereby leading to a reaction field **E** (generated by the polarized solvent) that scales in proportion to $g(\epsilon)$, $\mathbf{E} = (2g(\epsilon)/a^3)\mu$.[70,72] Despite
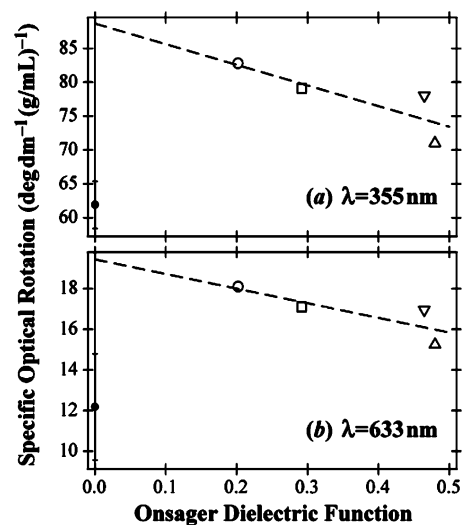

Figure 4. Distinct behavior of chiro-optical response for isolated and solvated species. The specific optical rotation of (R)-cis-pinane is plotted against the Onsager dielectric function, $g(\epsilon) = (\epsilon - 1)/(2\epsilon + 1)$, to contrast the behavior exhibited by isolated and solvated species. The solid circular symbols and associated error bars represent gas-phase ($\epsilon = 1.0$) CRDP measurements performed at excitation wavelengths of 355 (top panel) and 633 nm (bottom panel). The accompanying opened symbols show analogous solution-phase results interpolated from dilute cyclohexane (O, $\epsilon = 2.02$), di-n-butyl ether (□, $\epsilon = 3.06$), acetone (▽, $\epsilon = 20.7$), and acetonitrile (△, $\epsilon = 36.6$) polarimetric studies. The dashed line in each panel depicts the extrapolation of solution-phase response ($\epsilon > 1$) to the vapor-phase limit ($\epsilon = 1.0$).

explicit exclusion of first solvation shell effects in the cybotactic region,[69] such continuum-dielectric models have been found to provide reasonable descriptions for aprotic (sans hydrogen bonding) and nonaromatic (dipole-dominated) solvents that do not engage in specific solute−solvent interactions.

The Onsager dielectric function has been used to explore solvent effects exhibited by varied chemical processes (e.g., conformational equilibrium shifts,[73] barriers to internal rotation,[74] and activation energies for bimolecular reactions[75]), with plots analogous to those of Figure 4 enabling monotonic extrapolation of solution-phase ($\epsilon > 1$) results to their gas-phase ($\epsilon = 1$) counterparts. Analogous theoretical frameworks have been enlisted to describe the influence of nonspecific solvation upon frequency-dependent molecular properties, including vibrational and electronic spectra.[69,76] The solvents employed for the present investigations of nonresonant optical activity have been selected to span a significant portion of the accessible abscissa scale and to meet criteria imposed for fruitful exploitation of the dipolar reaction field model. Consequently, the ordinate intercepts deduced from linear regression analyses

would be expected to provide reasonable estimates for the chiro-optical response evoked from isolated solute molecules. Obviously, such predictions are not realized since CRDP measurements of $[\alpha]_{355nm}^{25°C}$ and $[\alpha]_{633nm}^{25°C}$ for solvent-free (R)-cis-pinane are found to be substantially smaller in magnitude than extrapolated (reaction field) values. Similar conclusions have been found for all of the chiral species examined by our polarimetric studies.[43]

The anomalous scaling with dielectric constant illustrated in Figure 4 suggests that a serious incongruity exists between specific rotation parameters acquired under solvated and isolated conditions, with the latter routinely displaying characteristics reminiscent of those found in solvents of high polarity. This unexpected result casts fundamental doubts on the relevance of comparisons often made between canonical (solution-based) measurements of nonresonant optical activity and ab initio predictions of corresponding solvent-free properties. Indeed, direct inspection of $[\alpha]_{355nm}^{25°C}$ and $[\alpha]_{633nm}^{25°C}$ values has shown that solvents possessing substantial dielectric constants (e.g., acetonitrile and acetone) consistently provide a better mimic of vapor-phase behavior than their less-polar counterparts (e.g., cyclohexane), a result that would appear to contradict conventional wisdom regarding the nature of attendant solute−solvent perturbations.

Solvent molecules long have been known to markedly influence both the magnitude and the sign of chiro-optical response.[10] In the case of flexible solutes such as epichlorohydrin, these observations commonly have been attributed to geometrical relaxation of the nuclear framework that results in the differential stabilization of specific conformers,[41,57,77,78] each of which can possess unique and, oftentimes, antagonistic behavior (cf., Tables 4 and 5). Nevertheless, as demonstrated succinctly by the methyloxirane data in Figure 1, even nominally rigid species can exhibit pronounced solvation phenomena that ultimately must be ascribed to attendant changes in the static and dynamic distribution of electron density. Some insight into the origins of these effects can be gleaned by considering the basic quantum mechanical framework developed for the description of natural optical activity.[9,11,16] Canonical theoretical treatments of CB and CD lead to definition of the scalar rotatory strength, ^{eg}R, which couples ground (electronic) state $|g\rangle$ to excited (electronic) state $|e\rangle$ under the simultaneous action of electric (E1) and magnetic (M1) dipole transitions. This quantity plays a role analogous to that of the oscillator strength in conventional spectroscopy and can be cast as a summation over diagonal elements (or trace) of the rotatory tensor, $^{eg}\mathbf{R}$:

$$^{eg}R = \text{Tr}[^{eg}\mathbf{R}] = \text{Im}\{\langle g|\hat{\boldsymbol{\mu}}^{(E1)}|e\rangle \cdot \langle e|\hat{\boldsymbol{\mu}}^{(M1)}|g\rangle\}$$
$$= \,^{eg}R_{xx} + \,^{eg}R_{yy} + \,^{eg}R_{zz} \qquad (7)$$

where formally $^{eg}R_{\beta\beta'} = \text{Im}\{\langle g|\hat{\mu}_\beta^{(E1)}|e\rangle\langle e|\hat{\mu}_{\beta'}^{(M1)}|g\rangle\}$. By exploiting time-dependent perturbation theory to model the chiro-optical response evoked by monochromatic light of angular frequency ω, the natural optical activity supported by an isotropic chiral medium can be described uniformly in terms of the frequency-dependent $E1 - M1$ linear susceptibility tensor, $\chi^{(1)}(\omega)$:[9,79]

$$\chi_{\beta\beta'}^{(1)}(\omega) =$$
$$\frac{1}{\epsilon_0 \hbar}\sum_{e\neq g}\left[\frac{\langle g|\hat{\mu}_\beta^{(E1)}|e\rangle\langle e|\hat{\mu}_{\beta'}^{(M1)}|g\rangle}{\omega_{eg} - \omega - i\Gamma_{eg}} + \frac{\langle g|\hat{\mu}_{\beta'}^{(M1)}|e\rangle\langle e|\hat{\mu}_\beta^{(E1)}|g\rangle}{\omega_{eg} + \omega + i\Gamma_{eg}}\right] \quad (8)$$

where the summation is performed over all electronically excited manifolds. While the rest frequency for the $|e\rangle \leftrightarrow |g\rangle$ resonance follows from the difference in unperturbed energies for the participating states, $\omega_{eg} = (E_e - E_g)/\hbar$, the corresponding dephasing rate can be expressed as the average value of attendant depopulation rates, $\Gamma_{eg} = 1/2(\Gamma_{ee} + \Gamma_{gg}) + \Gamma'_{eg}$, with an additional Γ'_{eg} term stemming from pure-dephasing processes (e.g., elastic collisions) that disrupt molecular coherences but do not affect molecular populations.[80]

The CB phenomena that dominate under nonresonant conditions ($\omega \neq \omega_{eg}$) are characterized by a difference in refractive index for left-circular and right-circular helicity states, $\Delta n(\omega) = n_L(\omega) - n_R(\omega)$, with the angle of linear polarization rotation per unit path length of chiral medium being defined by $\phi(\omega) = (\omega/2c)\Delta n(\omega)$.[9,11] The requisite value of $\Delta n(\omega)$ for such optical activity calculations follows from the imaginary part of the trace over $\chi^{(1)}(\omega)$:[79]

$$\Delta n(\omega) \propto \text{Im}\{\text{Tr}[\chi^{(1)}(\omega)]\}$$
$$= \text{Im}[\chi_{xx}^{(1)}(\omega) + \chi_{yy}^{(1)}(\omega) + \chi_{zz}^{(1)}(\omega)]$$
$$\propto \frac{1}{\epsilon_0\hbar}\sum_{e\neq g}\left[\frac{\omega_{eg} - \omega}{(\omega_{eg} - \omega)^2 + \Gamma_{eg}^2} - \frac{\omega_{eg} + \omega}{(\omega_{eg} + \omega)^2 + \Gamma_{eg}^2}\right]^{eg}R$$
$$\xrightarrow{\Gamma_{eg}=0} \frac{2\omega}{\epsilon_0\hbar}\sum_{e\neq g}\frac{^{eg}R}{\omega_{eg}^2 - \omega^2} \qquad (9)$$

where the final expression, often invoked in the limit of large detuning ($\omega \ll \omega_{eg}$), arises from neglect of dephasing processes (the infinite lifetime approximation). As highlighted by the summation over *all* excited states, $\Delta n(\omega)$ and $\phi(\omega)$ are composite molecular properties that reflect the dynamical response of the entire electron distribution to oscillating electromagnetic fields. The CD phenomena that dominate under conditions of resonant excitation ($\omega \approx \omega_{eg}$) can be treated in a similar fashion,[9,79] with the polarization ellipticity of light emerging from a chiral sample being proportional to the real part of the trace over $\chi^{(1)}(\omega)$.

By excluding cooperative mechanisms (e.g., the formation of chiral solvation shells[81] or the action of solvent-mediated vibronic coupling[82]) and focusing on the isolated-molecule behavior embodied in eqs 7−9, solute−solvent interactions can be expected to perturb the transition energies ($\hbar\omega_{eg}$), dephasing rates (Γ_{eg}), and rotatory strengths (^{eg}R) for individual excited states. Aside from altering the locations and (signed) amplitudes of resonant CD features, such effects will mediate the role that each $|e\rangle$ manifold plays in constituting the composite property of nonresonant CB. The diffuse nature of Rydberg states should make them especially susceptible to solvent-induced energy shifts (solvatochroism affecting ω_{eg}) and dephasing processes (homogeneous broadening affecting Γ_{eg}), a fact documented by the collisional-quenching techniques long used to discriminate (gas-phase) Rydberg absorption bands from their valence counterparts.[83] From this perspective, the glaring discrepancies uncovered between vapor-phase and solution-phase specific rotation parameters can be attributed, in part, to the selective exclusion, dampening, and/or frequency-shifting of contributions arising from manifolds that possess substantial Rydberg character (which should be pervasive in regimes of high electronic excitation). Theoretical corroboration of this assertion might follow from a state-by-state decomposition of ORD curves; however, modern ab initio calculations seldom perform the

summation of eq 9 explicitly, relying instead on a time-dependent linear response formalism[84] to efficiently evaluate elements of the frequency-dependent $E1 - M1$ polarizability tensor, $\mathbf{G}'(\omega)$[79]

$$G'_{\beta\beta'}(\omega) = -\text{Im}\{\chi^{(1)}_{\beta\beta'}(\omega)\} \tag{10}$$

which provides the needed information for both ORD and CD predictions (the latter following from the residue of $G'_{\beta\beta'}(\omega)$ as $\omega \rightarrow \omega_{eg}$). Furthermore, quantum chemical treatments of chiro-optical response seldom incorporate dephasing effects explicitly,[28] with most simulations of resonant (CD) spectral features instead relying on phenomenological line shape functions scaled by computed values of the rotatory strength. While such deficiencies can be attributed to the lack of viable methods for evaluating requisite Γ_{eg} parameters, the implication of dissipation processes and electronic parentage as potential mediators for the environmental perturbation of nonresonant optical activity must not be discounted. This remains an open issue for future research endeavors, as do the attendant roles played by intrinsic (vibrational)[43,63,77,85] and extrinsic (conformational) structural nonrigidity.

V. Summary and Conclusions

The nonresonant optical activity (or circular birefringence) of prototypical organic compounds has been interrogated under complementary solution-phase and vapor-phase conditions, with the latter studies being performed at two discrete excitation wavelengths (355 and 633 nm) by means of the ultrasensitive cavity ring-down polarimetry (CRDP) technique.[38,39] Specific (linear) polarization rotation parameters (in canonical units of deg dm^{-1} (g/mL)$^{-1}$) have been measured for a variety of isolated (solvent-free) chiral species, including both rigid and nonrigid members of the terpene, epoxide, and alkane/alkene families. High-level ab initio calculations, employing extensive GIAO basis sets in conjunction with the time-dependent linear response formalism of density functional theory, have been exploited to elucidate the structural and electronic origins of observed chiro-optical properties.

Direct comparison of analogous solution-phase and vapor-phase CB measurements has provided a trenchant glimpse of the environmental perturbations that mediate chiro-optical properties in condensed media. For flexible solute molecules (e.g., epichlorohydrin), these observations commonly can be attributed to the differential solvation/stabilization of individual conformers, each of which makes a unique and, oftentimes, antagonistic contribution to the total optical activity. In contrast, the pronounced solvation effects exhibited by nominally rigid species (e.g., methyloxirane) must reflect attendant changes in the static and dynamic distribution of electron density, with specific rotation parameters extracted under isolated (solvent-free) conditions surprisingly found to resemble those obtained in solvents of high polarity. Such anomalous behavior is the subject of ongoing investigations; however, the basic theory governing chiral matter-field interactions suggests that solvent-induced quenching and/or shifting of certain excited states (i.e., diffuse manifolds of substantial Rydberg character) might play a pivotal role. On the other hand, even in cases where the potential energy landscape is dominated by a single configuration of the nuclear framework, the influence of vibrational (zero-point) motion upon chiro-optical response remains a largely unexplored issue.[43,63,77,85]

By lifting the veil of solvation and revealing the intrinsic response evoked from isolated (solvent-free) molecules, the present investigations of nonresonant optical activity can fill several notable voids in our understanding of chiro-optical phenomena. On one hand, differences uncovered between the solution-phase and vapor-phase CB of rigid species yield clear evidence for solute−solvent perturbations, which are found to be surprisingly strong and pervasive even in the case of nonspecific coupling. This unequivocal resolution of environmental effects provides an essential ingredient for systematically improving current theoretical models of chiral solvation processes, a prerequisite for any viable attempt to address the complications incurred by conformational flexibility. At the same time, the interrogation of isolated-molecule behavior under well-defined experimental conditions furnishes the body of refined data needed to critically assess burgeoning ab initio calculations of optical activity and to impartially gauge their potential for assigning absolute stereochemical configuration. In pursuit of such goals, ongoing work in our laboratories has targeted a variety of judiciously selected compounds that embody physical/chemical characteristics and structural motifs designed to elucidate the electronic provenance of chiro-optical behavior, as mediated by structural nonrigidity (conformational flexibility and vibrational motion) and solute−solvent interactions. Related efforts have been directed toward further development of the CRDP methodology, including enhanced wavelength versatility and agility, as well as the ability to probe resonant CD features in rarefied media.

References and Notes

(1) Mislow, K. *Top. Stereochem.* **1999**, *22*, 1. *Chirality: Physical Chemistry*; Hicks, J. M., Ed.; American Chemical Society: Washington, D. C., 2002. *Chirality in Natural and Applied Science*; Lough, W. J., Wainer, I. W., Eds.; CRC Press LLC/Blackwell Science Ltd.: Boca Raton, FL, 2002.

(2) Eliel, E. L.; Wilen, S. H.; Doyle, M. P. *Basic Organic Stereochemistry*; John Wiley and Sons: New York, 2001.

(3) Barron, L. D. *J. Am. Chem. Soc.* **1979**, *101*, 269. Barron, L. D. *Chem. Phys. Lett.* **1986**, *123*, 423. Barron, L. D. *Chem. Phys. Lett.* **1994**, *221*, 311. Barron, L. D. True and False Chirality, CP Violation, and the Breakdown of Microscopic Reversibility in Chiral Molecular and Elementary Particle Processes. In *AIP Conference Proceedings 379 (Physical Origin of Homochirality in Life)*; Cline, D. B., Ed.; AIP Press: Woodbury, NY, 1995; Vol. 379; p 162. MacDermott, A. J. *Enantiomer* **2000**, *5*, 153. Avalos, M.; Babiano, R.; Cintas, P.; Jimenez, J. L.; Palacios, J. C. *Tetrahedron-Asym.* **2000**, *11*, 2845. Quack, M. *Angew. Chem., Int. Ed.* **2002**, *41*, 4618. Quack, M. *Chimica* **2003**, *57*, 147. Crassous, J.; Monier, F.; Dutasta, J.-P.; Ziskind, M.; Daussy, C.; Grain, C.; Chardonnet, C. *Chem. Phys. Chem.* **2003**, *4*, 541.

(4) Noyori, R.; Kitamura, M. *Angew. Chem., Int. Ed. Engl.* **1991**, *30*, 49. Inoue, Y. *Chem. Rev.* **1992**, *92*, 741. Guillaneux, D.; Zhao, S.-H.; Samuel, O.; Rainford, D.; Kagan, H. B. *J. Am. Chem. Soc.* **1994**, *116*, 9430. Huck, N. P. M.; Jager, W. F.; de Lange, B.; Feringa, B. L. *Science* **1996**, *273*, 1686. Huck, N. P. M.; Jager, W. F.; de Lange, B.; Feringa, B. L. *Science* **1997**, *276*, 341. Inoue, Y.; Matsushima, E.; Wada, T. *J. Am. Chem. Soc.* **1998**, *120*, 10687. Feringa, B. L.; van Delden, R. A. *Angew. Chem., Int. Ed.* **1999**, *38*, 3418. Inoue, Y.; Wada, T.; Asaoka, S.; Sato, H.; Pete, J.-P. *Chem. Commun.* **2000**, *2000*, 251. Mikami, K.; Yamanaka, M. *Chem. Rev.* **2003**, *103*, 3369.

(5) Bonner, W. A. *Top. Stereochem.* **1988**, *18*, 1. Bonner, W. A. The Quest for Chirality. In *AIP Conference Proceedings 379 (Physical Origin of Homochirality in Life)*; Cline, D. B., Ed.; American Institute of Physics: Woodbury, NY, 1996; Vol. 379; p 17. Cline, D. B. On the Determination of the Physical Origin of Homochirality in Life. In *AIP Conference Proceedings 379 (Physical Origin of Homochirality in Life)*; Cline, D. B., Ed.; American Institute of Physics Press: Woodbury, NY, 1996; Vol. 379; p 266. Bonner, W. A. *Chirality* **2000**, *12*, 114. MacDermott, A. J. The Origin of Biomolecular Chirality. In *Chirality in Natural and Applied Science*; Lough, W. J., Wainer, I. W., Eds.; Blackwell Science: Oxford, U.K., 2002; p 23.

Optical Activity in the Vapor Phase

J. Phys. Chem. A, Vol. 109, No. 51, 2005 **11763**

(6) Bijvoet, J. M.; Peerdeman, A. F.; van Bommel, A. J. *Nature (London)* **1951**, *168*, 271. Bijvoet, J. M. *Endeavour* **1955**, *14*, 71. Saito, Y. X-ray and Neutron Diffraction. In *Spectroscopy and Structure of Metal Chelate Compounds*; Nakamoto, K., Ed.; John Wiley and Sons: New York, 1968; p 1. Saito, Y. *Coord. Chem. Rev.* **1974**, *13*, 305. Schultze-Rhonhof, E. *Method Chim.* **1974**, *1*, 546. Flack, H. D.; Bernardinelli, G. *Acta Crystallogr. A* **1999**, *A55*, 908.

(7) Rinaldi, P. L. *Prog. Nucl. Magn. Reson. Spectrosc.* **1982**, *15*, 291. Seco, J. M.; Quinoa, E.; Riguera, R. *Tetrahedron-Asym.* **2001**, *12*, 2915. Seco, J. M.; Quinoa, E.; Riguera, R. *Chem. Rev.* **2004**, *104*, 17. Wenzel, T. J.; Wilcox, J. D. *Chirality* **2003**, *15*, 256.

(8) Dearden, D. V.; Liang, Y.; Nicoll, J. B.; Kellersberger, K. A. *J. Mass Spectrom.* **2001**, *36*, 989. König, W. A.; Hochmuth, D. H. *J. Chromatogr. Sci.* **2004**, *42*, 423.

(9) Wagnière, G. H. *Linear and Nonlinear Optical Properties of Molecules*; VCH Publishers: New York, 1993.

(10) *Circular Dichroism: Principles and Applications*; Berova, N.; Nakanishi, K.; Woody, R. W., Eds.; John Wiley and Sons: New York, 2000. Eliel, E. L.; Wilen, S. H.; Doyle, M. P. Chapter 12: Chiroptical Properties. In *Basic Organic Stereochemistry*; Johns Wiley and Sons: New York, 2001.

(11) Barron, L. D. *Molecular Light Scattering and Optical Activity*, 2nd ed.; Cambridge University Press: Cambridge, U.K., 2004.

(12) Barron, L. D.; Hecht, L. Chapter 23: Vibrational Raman Optical Activity: From Fundamentals to Biochemical Applications. In *Circular Dichroism*; Berova, N., Nakanishi, K., Woody, R. W., Eds.; John Wiley and Sons: New York, 2000; p 667. Barron, L. D.; Blanch, E. W.; Bell, A. F.; Syme, C. D.; Hecht, L.; Day, L. A. Chapter 3: New Insights into Solution Structure and Dynamics of Proteins, Nucleic Acids, and Viruses from Raman Optical Activity. In *Chirality: Physical Chemistry*; Hicks, J. M., Ed.; American Chemical Society: Washington, DC, 2002; p 34.

(13) Stephens, P. J.; Lowe, M. A. *Annu. Rev. Phys. Chem.* **1985**, *36*, 213. Nafie, L. A. *Annu. Rev. Physiol. Chem.* **1997**, *48*, 357. Nafie, L. A.; Freedman, T. B. Chapter 4: Vibrational Optical Activity Theory. In *Circular Dichroism*; Berova, N., Nakanishi, K., Woody, R. W., Eds.; John Wiley and Sons: New York, 2000; p 97. Stephens, P. J.; Devlin, F. J.; Aamouche, A. Chapter 2: Determination of the Structures of Chiral Molecules Using Vibrational Circular Dichroism Spectroscopy. In *Chirality: Physical Chemistry*; Hicks, J. M., Ed.; American Chemical Society: Washington, DC, 2002; p 18. Freedman, T. B.; Cao, X.; Dukor, R. A.; Nafie, L. A. *Chirality* **2003**, *15*, 743.

(14) Polavarapu, P. L. *Chirality* **2002**, *14*, 768.

(15) Born, M. *Z. Phys.* **1915**, *16*, 251. Oseen, C. W. *Ann. Phys.* **1915**, *48*, 1. Gray, F. *Phys. Rev.* **1916**, *7*, 472. Rosenfeld, L. *Z. Physik* **1928**, *52*, 161. Born, M. *Proc. R. Soc. A* **1935**, *150*, 84.

(16) Condon, E. U. *Rev. Mod. Phys.* **1937**, *9*, 432.

(17) Delvin, F. J.; Stephens, P. J.; Cheeseman, J. R.; Frisch, M. J. *J. Phys. Chem. A* **1997**, *101*, 6322. Delvin, F. J.; Stephens, P. J.; Cheeseman, J. R.; Frisch, M. J. *J. Phys. Chem. A* **1997**, *101*, 9912. Stephens, P. J.; Devlin, F. J.; Cheeseman, J. R.; Frisch, M. J.; Rosini, C. *Org. Lett.* **2002**, *4*, 4595.

(18) Cheeseman, J. R.; Frisch, M. J.; Delvin, F. J.; Stephens, P. J. *J. Phys. Chem. A* **2000**, *104*, 1039.

(19) Stephens, P. J.; Delvin, F. J.; Cheeseman, J. R.; Frisch, M. J. *J. Phys. Chem. A* **2001**, *105*, 5356.

(20) Mennucci, B.; Tomasi, J.; Cammi, R.; Cheeseman, J. R.; Frisch, M. J.; Devlin, F. J.; Gabriel, S.; Stephens, P. J. *J. Phys. Chem. A* **2002**, *106*, 6102.

(21) Stephens, P. J.; Delvin, F. J.; Cheeseman, J. R.; Frisch, M. J.; Bortolini, O.; Besse, P. *Chirality* **2003**, *15*, S57. McCann, D. M.; Stephens, P. J.; Cheeseman, J. R. *J. Org. Chem.* **2004**, *69*, 8709. Stephens, P. J.; McCann, D. M.; Cheeseman, J. R.; Frisch, M. J. *Chirality* **2005**, *17*, S52.

(22) Kondru, R. K.; Lim, S.; Wipf, P.; Beratan, D. N. *Chirality* **1997**, *9*, 469. Kondru, R. K.; Wipf, P.; Beratan, D. N. *Science* **1998**, *282*, 2247. Kondru, R. K.; Wipf, P.; Beratan, D. N. *J. Am. Chem. Soc.* **1998**, *120*, 2204. Kondru, R. K.; Wipf, P.; Beratan, D. N. *J. Phys. Chem. A* **1999**, *103*, 6603. Beratan, D. N.; Kondru, R. K.; Wipf, P. Optical Activity: From Structure−Function to Structure Prediction. In *Chirality: Physical Chemistry*; Hicks, J. M., Ed.; American Chemical Society: Washington, DC, 2002; Vol. 810; p 104. Goldsmith, M.-R.; Jayasuriya, N.; Beratan, D. N.; Wipf, P. *J. Am. Chem. Soc.* **2003**, *125*, 15696. Goldsmith, M.-R.; Jayasuriya, N.; Beratan, D. N.; Wipf, P. *J. Am. Chem. Soc.* **2003**, *126*, 9464.

(23) Grimme, S. *Chem. Phys. Lett.* **1996**, *259*, 128. Pulm, F.; Schramm, J.; Hormes, J.; Grimme, S.; Peyerimhoff, S. D. *Chem. Phys.* **1997**, *224*, 143. Furche, F.; Ahlrichs, R.; Wachsmann, C.; Weber, E.; Sobanski, A.; Vögtle, F.; Grimme, S. *J. Am. Chem. Soc.* **2000**, *122*, 1717. Grimme, S. *Chem. Phys. Lett.* **2001**, *339*, 380. Grimme, S.; Furche, F.; Ahlrichs, R. *Chem. Phys. Lett.* **2002**, *361*.

(24) Diedrich, C.; Causemann, S.; Grimme, S. *J. Comput. Methods Sci. Eng.* **2004**, *4*, 293.

(25) Polavarapu, P. L. *Tetrahedron: Asym.* **1997**, *8*, 3397. Polavarapu, P. L. *Mol. Phys.* **1997**, *91*, 551. Polavarapu, P. L.; Chakraborty, D. K. *J. Am. Chem. Soc.* **1998**, *120*, 6160. Polavarapu, P. L.; Zhao, C. *Chem. Phys.*

Lett. **1998**, *296*, 105. Polavarapu, P. L.; Zhao, C. *J. Am. Chem. Soc.* **1999**, *121*, 246. Polavarapu, P. L.; Chakraborty, D. K. *Chem. Phys.* **1999**, *240*, 1. Polavarapu, P. L. *Angew. Chem., Int. Ed.* **2002**, *41*, 4544.

(26) Polavarapu, P. L.; Chakraborty, D. K.; Ruud, K. *Chem. Phys. Lett.* **2000**, *319*, 595.

(27) Pecul, M.; Ruud, K.; Helgaker, T. *Chem. Phys. Lett.* **2004**, *388*, 110.

(28) Norman, P.; Ruud, K.; Helgaker, T. *J. Chem. Phys.* **2004**, *120*, 5027.

(29) Pecul, M.; Marchesan, D.; Ruud, K.; Coriani, S. *J. Chem. Phys.* **2005**, *122*, 1.

(30) Ruud, K.; Helgaker, T. *Chem. Phys. Lett.* **2002**, *352*, 533. Ruud, K.; Stephens, P. J.; Delvin, F. J.; Taylor, P. R.; Cheeseman, J. R.; Frisch, M. J. *Chem. Phys. Lett.* **2003**, *373*, 606.

(31) Tam, M. C.; Russ, N. J.; Crawford, T. D. *J. Chem. Phys.* **2004**, *121*, 3550.

(32) Crawford, T. D.; Owens, L. S.; Tam, M. C.; Schreiner, P. R.; Koch, H. *J. Am. Chem. Soc.* **2005**, *127*, 1368.

(33) Kongsted, J.; Pedersen, T. B.; Strange, M.; Osted, A.; Hansen, A. E.; Mikkelsen, K. V.; Pawlowski, F.; Jørgensen, P.; Hättig, C. *Chem. Phys. Lett.* **2005**, *401*, 385.

(34) Giorgio, E.; Rosini, C.; Viglione, R. G.; Zanasi, R. *Chem. Phys. Lett.* **2003**, *376*, 452.

(35) Giorgio, E.; Minichino, C.; Viglione, R. G.; Zanasi, R.; Rosini, C. *J. Org. Chem.* **2003**, *68*, 5186.

(36) Giorgio, E.; Viglione, R. G.; Zanasi, R.; Rosini, C. *J. Am. Chem. Soc.* **2004**, *126*, 12968.

(37) Carnell, M.; Peyerimhoff, S. D.; Breest, A.; Gödderz, K. H.; Ochmann, P.; Hormes, J. *Chem. Phys. Lett.* **1991**, *180*, 477. Carnell, M.; Peyerimhoff, S. D. *Chem. Phys.* **1994**, *183*, 37. Carnell, M.; Peyerimhoff, S. D. *Chem. Phys.* **1994**, *179*, 385.

(38) Müller, T.; Wiberg, K. B.; Vaccaro, P. H. *J. Phys. Chem. A* **2000**, *104*, 5959. Müller, T.; Wiberg, K. B.; Vaccaro, P. H. *Rev. Sci. Instrum.* **2002**, *73*, 1340.

(39) Müller, T.; Wiberg, K. B.; Vaccaro, P. H.; Cheeseman, J. R.; Frisch, M. J. *J. Opt. Soc. Am. B* **2002**, *19*, 125.

(40) Scherer, J. J.; Paul, J. B.; O'Keefe, A.; Saykally, R. J. *Chem. Rev.* **1997**, *97*, 25. Wheeler, M. D.; Newman, S. M.; Orr-Ewing, A. J.; Ashfold, M. N. R. *J. Chem. Soc., Faraday Trans.* **1998**, *94*, 337. Berden, G.; Peeters, R.; Meijer, G. *Int. Rev. Phys. Chem.* **2000**, *19*, 565. Vallance, C. *New J. Chem.* **2005**, *29*, 867.

(41) Polavarapu, P. L.; Petrovic, A.; Wang, F. *Chirality* **2003**, *15*, S143. Polavarapu, P. L.; Petrovic, A.; Wang, F. *Chirality* **2003**, *15*, 801.

(42) Hauptman, E.; Fagan, P. J.; Marshall, W. *Organometallics* **1999**, *18*, 2061.

(43) Wiberg, K. B.; Wang, Y.-G.; Wilson, S. M.; Vaccaro, P. H.; Cheeseman, J. R. *J. Phys. Chem. A* **2005**, *109*, 3448.

(44) Goodwin, D. G.; Hudson, H. R. *J. Chem Soc. B* **1968**, *11*, 1333.

(45) Constantin, G.; Ville, G. *Bull. Soc. Chim. Fr.* **1971**, *8*, 2974. Magid, R. M.; Fuchey, O. S.; Johnson, W. L.; Allen, T. G. *J. Org. Chem.* **1979**, *44*, 359.

(46) Frisch, M. J.; Trucks, G. W.; Schlegel, H. B.; Scuseria, G. E.; Robb, M. A.; Cheeseman, J. R.; Montgomery, J.; J. A.; Vreven, T.; Kudin, K. N.; Burant, J. C.; Millam, J. M.; Iyengar, S. S.; Tomasi, J.; Barone, V.; Mennucci, B.; Cossi, M.; Scalmani, G.; Rega, N.; Petersson, G. A.; Nakatsuji, H.; Hada, M.; Ehara, M.; Toyota, K.; Fukuda, R.; Hasegawa, J.; Ishida, M.; Nakajima, T.; Honda, Y.; Kitao, O.; Nakai, H.; Klene, M.; Li, X.; Knox, J. E.; Hratchian, H. P.; Cross, J. B.; Bakken, V.; Adamo, C.; Jaramillo, J.; Gomperts, R.; Stratmann, R. E.; Yazyev, O.; Austin, A. J.; Cammi, R.; Pomelli, C.; Ochterski, J. W.; Ayala, P. Y.; Morokuma, K.; Voth, G. A.; Salvador, P.; Dannenberg, J. J.; Zakrzewski, V. G.; Dapprich, S.; Daniels, A. D.; Strain, M. C.; Farkas, O.; Malick, D. K.; Rabuck, A. D.; Raghavachari, K.; Foresman, J. B.; Ortiz, J. V.; Cui, Q.; Baboul, A. G.; Clifford, S.; Cioslowski, J.; Stefanov, B. B.; Liu, G.; Liashenko, A.; Piskorz, P.; Komaromi, I; Martin, R. L.; Fox, D. J.; Keith, T.; Al-Laham, M. A.; Peng, C. Y.; Nanayakkara, A.; Challacombe, M.; Gill, P. M. W.; Johnson, B.; Chen, W.; Wong, M. W.; Gonzalez, C.; Pople, J. A. Gaussian 03, Revision C.02. Gaussian, Inc.: Wallingford, CT, 2004.

(47) Kliger, D. S.; Lewis, J. W.; Randall, C. E. *Polarized Light in Optical Spectroscopy*; Academic Press: Boston, MA, 1990.

(48) Slichter, C. P. *Principles of Magnetic Resonance*, 3rd ed.; Springer-Verlag: Berlin, 1990.

(49) Shen, Y. R. *The Principles of Nonlinear Optics*; John Wiley and Sons: New York, 1984. Butcher, P. N.; Cotter, D. *The Elements of Nonlinear Optics*; Cambridge University Press: Cambridge, U.K., 1990. Boyd, R. W. *Nonlinear Optics*; Academic Press: Boston, 1992. Mukamel, S. *Principles of Nonlinear Optical Spectroscopy*; Oxford University Press: New York, 1995.

(50) Power, E. A. *J. Chem. Phys.* **1975**, *63*, 1348. Tinoco, I., Jr. *J. Chem. Phys.* **1975**, *62*, 1006. Andrews, D. L. *Chem. Phys.* **1976**, *16*, 419. Wagnière, G. *J. Chem. Phys.* **1982**, *77*, 2786. Sztucki, J.; Strek, W. *J. Chem. Phys.* **1986**, *85*, 5547. Meath, W. J.; Power, E. A. *J. Mod. Opt.* **1989**, *36*, 977.

Gunde, K. E.; Burdick, G. W.; Richardson, F. S. *Chem. Phys.* **1996**, *208*, 195. Gunde, K. E.; Burdick, G. W.; Richardson, F. S. *Chem. Phys.* **1996**, *210*, 515.

(51) Atkins, P. W.; Barron, L. D. *Proc. R. Soc. A* **1968**, *306*, 119. Kielich, S. *Acta Phys. Pol.* **1969**, *35*, 861. Power, E. A. Developments in the Theory of Multiphoton Absorption by Molecules (Bound-Bound): Applications of Chiroptic Character. In *New Frontiers in Quantum Electrodynamics and Quantum Optics*; NATO ASI Series, Series B: Physics 232; Barut, A. D., Ed.; Plenum Press: New York, 1990; p 153.

(52) Vlasov, D. V.; Zaitsev, V. P. *JETP Lett.* **1971**, *14*, 112. Gedanken, A.; Tamir, M. *Rev. Sci. Instrum.* **1987**, *58*, 950. Markowicz, P. P.; Samoc, M.; Cerne, J.; Prasad, P. N.; Pucci, A.; Ruggeri, G. *Opt. Express* **2004**, *12*, 5209.

(53) Cameron, R.; Tabisz, G. C. *Mol. Phys.* **1997**, *90*, 159.

(54) Swalen, J. D.; Herschbach, D. R. *J. Chem. Phys.* **1957**, *27*, 100.

(55) Kumata, Y.; Furukawa, J.; Fueno, T. *Bull. Chem. Soc. Jpn.* **1970**, *43*, 3920.

(56) Hayashi, M.; Hamo, K.; Ohno, K.; Murata, H. *Bull. Chem. Soc. Jpn.* **1972**, *45*, 949. Charles, S. W.; Jones, G. I. L.; Owen, N. L. *J. Mol. Struct.* **1974**, *20*, 83. Aroney, M. J.; Calderbank, K. E.; Stootman, H. J. *Aust. J. Chem.* **1978**, *31*, 2303. Fujiwara, F. G.; Chang, J. C.; Kim, H. *J. Mol. Struct.* **1977**, *41*, 177. Mohammadi, M. A.; Brooks, W. V. F. *J. Mol. Spectrosc.* **1978**, *73*, 353. Mohammadi, M. A.; Brooks, W. V. F. *J. Mol. Spectrosc.* **1979**, *78*, 89. Shen, Q. *J. Mol. Struct.* **1985**, *130*, 275. Lee, M. J.; Hur, S. W.; Durig, J. R. *J. Mol. Struct.* **1998**, *444*, 99.

(57) Wang, F.; Polavarapu, P. L. *J. Phys. Chem. A* **2000**, *104*, 6189.

(58) Biot, J.-B. *Mem. Acad. R. Sci. Inst. Fr.* **1817**, *2*, 41. Gernez, D. D. *Ann. Sci. Ec. Norm. Sup.* **1864**, *1*, 1. Guye, P.-A.; do Amaral, A.-P. *Arch. Sci. Phys. Nat.* **1895**, *33*, 513. Lowry, T. M.; Gore, H. K. *Proc. R. Soc. London, Ser. A* **1931**, *A135*, 13. Poirson, J.; Vallet, M.; Bretenaker, F.; Le Floch, A.; Thépot, J.-Y. *Anal. Chem.* **1998**, *70*, 4636.

(59) Bartlett, R. J. Chapter 16: Coupled-Cluster Theory: An Overview of Recent Developments. In *Modern Electronic Structure Theory*; Yarkony, D. R., Ed.; World Scientific: Singapore, 1995; Vol. 2; p 1047. Crawford, T. D.; Schaefer, H. F. Chapter 2: An Introduction to Coupled Cluster Theory for Computational Chemists. In *Reviews in Computational Chemistry*; Lipkowitz, K. B., Boyd, D. B., Eds.; VCH Publishers: New York, 2000; Vol. 14; p 33.

(60) Parr, R. G.; Yang, W. *Density-Functional Theory of Atoms and Molecules*; Oxford University: New York, 1989.

(61) Casida, M. E. Time-Dependent Density-Functional Response Theory for Molecules. In *Recent Advances in Density Functional Methods, Part I.*; Chong, D. P., Ed.; World Scientific: Singapore, 1995; Vol. 1; p 155. Bauernschmitt, R.; Ahlrichs, R. *Chem. Phys. Lett.* **1996**, *256*, 454.

(62) Lee, T. J.; Scuseria, G. E. Achieving Chemical Accuracy with Coupled-Cluster Theory. In *Quantum Mechanical Electronic Structure Calculations with Chemical Accuracy*; Langhoff, S. R., Ed.; Kluwer Academic Publishers: Dordrecht, The Netherlands, 1995; p 47. Helgaker, T.; Ruden, T. A.; Jørgensen, P.; Olsen, J.; Klopper, W. *J. Phys. Org. Chem.* **2004**, *17*, 913.

(63) Ruud, K.; Zanasi, R. *Angew. Chem., Int. Ed.* **2005**, *44*, 3594.

(64) Wiberg, K. B.; Wang, Y.-G.; Vaccaro, P. H.; Cheeseman, J. R.; Trucks, G.; Frisch, M. J. *J. Phys. Chem. A* **2004**, *108*, 32.

(65) Wolinski, K.; Hinton, J. F.; Pulay, P. *J. Am. Chem. Soc.* **1990**, *112*, 8251.

(66) Hameka, H. F. *Advanced Quantum Chemistry; Theory of Interactions between Molecules and Electromagnetic Fields*; Addison-Wesley Publishing Co.: Reading, MA, 1965.

(67) Helgaker, T.; Ruud, K.; Bak, K. L.; Jørgensen, P.; Olsen, J. *Faraday Discuss.* **1994**, *99*, 165.

(68) Wiberg, K. B. *J. Org. Chem.* **2003**, *68*, 9322.

(69) Tomasi, J.; Persico, M. *Chem. Rev.* **1994**, *94*, 2027. Cramer, C. J.; Truhlar, D. G. *Chem. Rev.* **1999**, *99*, 2161.

(70) Foresmann, J. B.; Keith, T. A.; Wiberg, K. B.; Snoonian, J.; Frisch, M. J. *J. Phys. Chem.* **1996**, *100*, 16098.

(71) Onsager, L. *J. Am. Chem. Soc.* **1936**, *58*, 1486.

(72) Wong, M. W.; Frisch, M. J.; Wiberg, K. B. *J. Am. Chem. Soc.* **1991**, *113*, 4776.

(73) Wiberg, K. B.; Keith, T. A.; Frisch, M. J.; Murko, M. *J. Phys. Chem.* **1995**, *99*, 9072.

(74) Wiberg, K. B.; Rablen, P. R.; Rush, D. J.; Keith, T. A. *J. Am. Chem. Soc.* **1995**, *117*, 4261. Wiberg, K. B.; Rush, D. J. *J. Am. Chem. Soc.* **2001**, *123*, 2038.

(75) Castejon, H.; Wiberg, K. B. *J. Am. Chem. Soc.* **1999**, *121*, 2139.

(76) Rao, C. N. R.; Singh, S.; Senthilnathan, V. P. *Chem. Soc. Rev.* **1976**, *5*, 297. Giorgini, M. G.; Fini, G.; Mirone, P. *J. Chem. Phys.* **1983**, *79*, 639. Suppan, P. *J. Photochem. Photobiol.* **1990**, *50*, 293. Kolling, O. W. *J. Phys. Chem.* **1992**, *96*, 6217. Linder, B. *J. Phys. Chem.* **1992**, *96*, 10708.

(77) Wiberg, K. B.; Vaccaro, P. H.; Cheeseman, J. R. *J. Am. Chem. Soc.* **2003**, *125*, 1888.

(78) Wiberg, K. B.; Wang, Y.-G.; Vaccaro, P. H.; Cheeseman, J. R.; Luderer, M. R. *J. Phys. Chem. A* **2005**, *109*, 3405.

(79) Pecul, M.; Ruud, K. The Ab Initio Calculation of Optical Rotation and Electronic Circular Dichroism. In *Advances in Quantum Chemistry*; Jensen, H., Ed.; Academic Press: New York, 2005; Vol. 50 (Response Theory and Molecular Properties), p xx.

(80) Berman, P. R. *Phys. Rev. A* **1972**, *5*, 927. Stenholm, S. *Foundations of Laser Spectroscopy*; John Wiley and Sons: New York, 1984.

(81) Fidler, J.; Roger, P. M.; Rodger, A. *J. Chem. Soc., Perkin Trans. 2* **1993**, 235. Fidler, J.; Rodger, P. M.; Rodger, A. *J. Am. Chem. Soc.* **1994**, *116*, 7266.

(82) Fischer, G. *Vibronic Coupling: The Interaction Between the Electronic and Nuclear Motions*; Academic Press: London, 1984. Ruiz-Lopez, M. F.; Rinaldi, D.; Rivail, J. L. *Chem. Phys.* **1986**, *110*, 403.

(83) Robin, M. B. *Higher Excited States of Polyatomic Molecules*; Academic Press: New York, 1974.

(84) Jørgensen, P.; Simons, J. *Second Quantization Based Methods in Quantum Chemistry*; Academic Press: New York, 1981. Olsen, J.; Jørgensen, P. *J. Chem. Phys.* **1985**, *82*, 3235. Jørgensen, P.; Jensen, H. J. A.; Olsen, J. *J. Chem. Phys.* **1988**, *89*, 3654.

(85) Ruud, K.; Taylor, P. R.; Astrand, P.-O. *Chem. Phys. Lett.* **2001**, *337*, 217.